International Journal of Innovative
Computing, Information and Control
Volume **10**, Number **3**, June **2014**

ICIC International ©2014 ISSN 1349-4198
pp. 1161-1178

EVALUATION OF PRODUCTION PROCESS USING MULTIMODE VIBRATION THEORY

Kenji Shirai[1] and Yoshinori Amano[2]

[1]Faculty of Information Culture
Niigata University of International and Information Studies
3-1-1, Mizukino, Nishi-ku, Niigata 950-2292, Japan
shirai@nuis.ac.jp

[2]Kyohnan Elecs Co., LTD.
8-48-2, Fukakusanishiura-cho, Fushimi-ku, Kyoto 612-0029, Japan
y_amano@kyohnan-elecs.co.jp

Received June 2013; revised October 2013

Abstract. *We introduce a potential field (a stochastic field) that corresponds to an electromagnetic field and evaluate a production process by means of multimode vibration theory. We clarified the nonlinear characteristics of the production process due to the standard deviation of workers within the production process. To maintain stable production process conditions, the process must operate within a phase transition range. Furthermore, the validation of evaluation based on the data throughput of the production process is presented.*

Keywords: Multimode vibration theory, Throughput, Delay propagation, Production process

1. **Introduction.** Several studies have addressed the problem of increasing the productivity of production processes used in the production industry [1, 2]. Moreover, in the field of production, various theories have been applied to improve and reform production processes and increase productivity.

In a previous study [3], we addressed the problem of reducing construction work and inventory in the steel industry. Specifically, we investigated the relationship between variations in the rate of construction and delivery rate. In this study, we perform analysis using the queuing model and apply log-normal distribution to model the system in the steel industry [3].

Moreover, several studies have reported approaches that lead to shorter lead times [4, 5]. From order products, lead time occurs on the work required preparation of the members for production.

Many aspects can potentially affect lead time. For example, from order products, the lead time from the start of development to the completion of a product is called the time-to-finish time, such as the work required preparation of the members for production equipments.

Moreover, several studies have focused on reducing customer's lead times. In [6], the author addresses the problem of reducing the production lead time.

In [7], the authors propose a method that increases both production efficiency and production of a greater diversity of products for customer use. Their proposed approach results in shortened lead times and reduces the uncertainty in demand. Their method captures the stochastic demand of customers and produces solutions by solving a nonlinear stochastic programming problem.

In summary, several studies have considered uncertainty and proposed practical approaches to shorten the lead time. The demand is treated as a stochastic variable and applied to mathematical programming. To our knowledge, previous studies have not treated lead time as a stochastic variable.

Because fluctuations in the supply chain and market demand and the changes in the production volume of suppliers are propagated to other suppliers, their effects are amplified. Therefore, because the amounts of stock are large, an increase or decrease of the suppliers' stock is modeled using differential equation. This differential equation is said as Billwhip model, which represents a stock congestion [8, 9].

The theory of constraints (TOC) describes the importance of avoiding bottlenecks in production processes [10]. When using production equipment, delays in one production step are propagated to the next. Hence, the use of production equipment may lead to delays. In this study, we apply a physical approach and regard each step as a continuous step. By applying this approach, we can mathematically analyze the delay of each step and obtain methods to address it. To the best of our knowledge, previous studies have not applied physical approaches to analyze delays.

In a previous study [12], we constructed a state in which the production density of each process corresponds to the physical propagation of heat [16]. Using this approach, we showed that a diffusion equation dominates the production process.

In other words, when minimizing the potential of the production field (stochastic field), the equation, which is defined by the production density function $S_i(x,t)$ and the boundary conditions, is described using the diffusion equation with advection to move in transportation speed ρ. The boundary condition means a closed system in the production field. The adiabatic state in thermodynamics represents the same state [12].

To achieve the goal of a production system, we propose using a mathematical model that focuses on the selection process and adaptation mechanism of the production lead time. We model the throughput time of the production demand/production system in the production stage using a stochastic differential equation of log-normal type, which is derived from its dynamic behavior. Using this model and the risk-neutral integral, we define and compute the evaluation equation for the compatibility condition of the production lead time. Furthermore, we apply the synchronization process and show that the throughput of the production process is reduced [13, 14].

To evaluate the production process, we propose the application of a production field (termed a stochastic field) that is analogous to a mechanical field in physics [12]. The behavior of production field is expressed as a partial differential equation describing a dynamic Hamilton-Jacobi field [23].

In addition, we clarify stable cycle conditions of nonlinear characteristic parameters in the production field of the production process. To date, nonlinearity in the rate of sales return in the production process has not been reported. However, the data analyzed in this study suggests that the rate of sales return can become nonlinear. The nonlinear element is the portion of production costs that cannot be directly attributed to sales.

Using this model, the evaluation equation for the compatibility condition production lead time is defined using the risk-neutral integral, thereby enabling the calculation of the evaluation equation for the above conditions. Furthermore, by the synchronization process, the throughput of the manufacturing process is reduced [13]. We also report that the difference between synchronous and asynchronous models is due to the volatility of the manufacturing process.

In addition, we perform experiments to clarify the reason for the difference between the asynchronous method, which causes a delay in the manufacturing process, and the synchronous method, which reduces the process throughput in manufacturing processes.

We indicate that a reduction in the volatility of synchronization leads to a decreased risk [14].

We clarify the nonlinearity of the production process that occurs due to the standard deviation (STD) of the workers. Within the regions of nonlinearity of the stochastic field of the production process, we clarify the stable conditions that maintain periodic solutions, for each cost and nonlinear parameter. Moreover, we establish that the nonlinear model is represented by a van der Pol differential equation. On the basis of actual data, we present that a planned production process, or increased throughput due to variations in the production process, operates in a manner similar to that of phase transitions in physics.

In this report, we present that the stable regions of nonlinearity of the production process correspond to regions of phase transition [20]. On the basis of actual throughput data, using an electrical circuit theory known as multimode vibration theory, we demonstrate that the factor causing reductions in production is throughput variations of work.

We introduce a potential field that corresponds to an electromagnetic field for analyzing the production process and apply multimode vibration theory to the potential field.

The present analysis has been conducted for increasing the production throughput. To the best of our knowledge, a dynamic multimode vibration model has not been mathematically applied to the production process previously. It is hoped that production operators can take advantage of the wealth of research results obtained from multiple vibration theory.

2. **Nonlinearity of the Production Process and the Potential Field.** Nonproductivity generates a static state in the production field. Transition to the dynamic state, modeled by the Hamilton-Jacobi equation, requires excitation energy, which increases the free energy of the system [23].

To retain profitable business, products must be continually input to the static field. At the same time, sustained input of order information is required. Figure 1 is an overview of the production field concept. The number of production units at each stage of a production unit i shifts over time. To function effectively, a production process requires a minimum number of personnel. This situation constitutes the shortest path problem. Production units can be considered to be physically located in mechanical fixtures. Production dynamics enable a company to profit from its business.

We consider that revenues are generated by the displacement of the potential in the production field. In other words, the entropy increase contributed by a production unit is another source of revenue. This is the principle of maximum entropy. Figure 2 illustrates

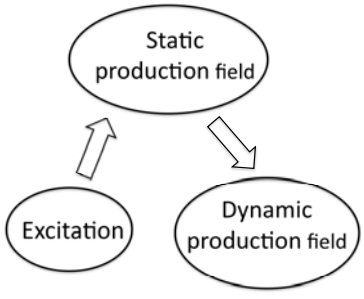

FIGURE 1. Overview of the production field concept

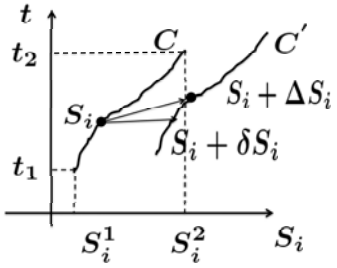

FIGURE 2. Transition from a lower-energy production process to the next higher-energy production process

the transition from a lower-energy production process (energy state C) to the next higher-energy process (energy state C').

Definition 2.1. *Production cost* $S_i(t)$

$$S_i(t) \equiv S_i^*(t) \pm \Delta S_i(t) \tag{1}$$

where the production cost $S_i^*(t)$ *incorporates cost fluctuations.*

We now derive the model equation that constrains the dynamic behavior of production costs.

As illustrated in Figure 3, profitability and production costs constitute the total potential of the system.

If the production field sets $\{S_i(t)\}$, $i = 1, \cdots, n$, introduce sustainable order information and excite the system having a sustainable target, then the process progresses from a static to a dynamic production field. The free energy of the process is increased by this transition. Costs are classified according to Figure 4. "Direct production cost" relates directly to production processes and represents labor and material costs.

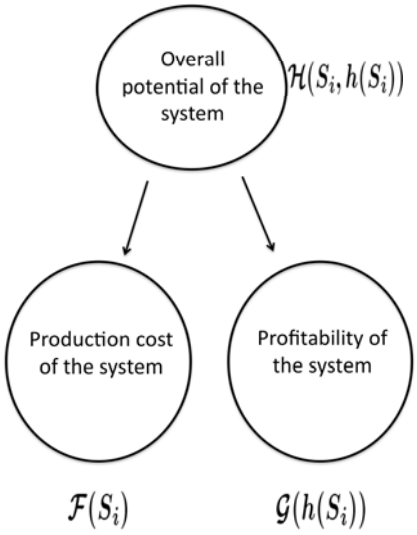

FIGURE 3. Overall potential of the system

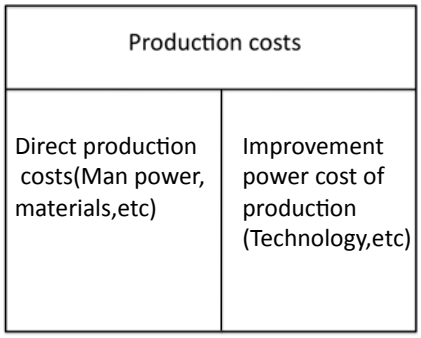

FIGURE 4. Two main divisions of production costs used in this study

Definition 2.2. *The rate of return specifies the variation of the production cost. That is, the rate of return* $h_{S_i}(t)$ *generated by improvement expenditure is as follows:*

$$h_{S_i}(t) \cong \frac{dS_i}{dt} \tag{2}$$

Definition 2.3. *Mixing potential energy* $(\mathcal{H}(S_i, h_{S_i}(t)))$

$$\mathcal{H}(S_i, h_{S_i}(t)) \equiv \mathcal{F}(S_i) + \mathcal{G}(h_{S_i}(t)) \tag{3}$$

where $\mathcal{G}(h_{S_i}(t))$ *denotes the production cost of improvement. The production cost is proportional to the rate of return. As an example, we consider the rate of return generated from technical proficiency. Because technical proficiency includes improvement power, it is hereafter referred to as "improvement power".*

In terms of $\mathcal{H}(S_i, h_{S_i})$, we have

$$k_s \frac{dS_i}{dt} = \frac{\partial H(S_i, h_{S_i})}{\partial S_i} \tag{4}$$

$$k_h \frac{dh_{S_i}}{dt} = \frac{\partial \mathcal{H}(S_i, h_{S_i})}{\partial h_{S_i}} \tag{5}$$

where k_s and k_h are constants. Equation (4) describes the time variation of direct production costs. Equation (5) represents the time variation of all rates of return. $\mathcal{H}(S_i, h_{S_i})$ is referred to as the mixing potential energy.

Definition 2.4. *Total rate of return* $h_T(S_i, t)$

$$h_T(S_i, t) \equiv \frac{\partial \mathcal{F}(S_i, h_{S_i})}{\partial S_i} + \mathcal{G}(h_{S_i}(t)) \tag{6}$$

where $\mathcal{G}(h_{S_i}(t))$ *represents the cumulative rate of returns generated by improvement expenditure in Equation (7).*

The total rate of return of a company in the production field is generated from both the time variation of the direct production cost and the "cumulative improvement cost for production". The time variation of production costs is assimilated into "production cost" in the production system. "Purchase cost" comprises the purchase of parts and other items used in the production. "Production cost with variation" is paid to external production contractors.

The cost also includes "transaction costs (sales volume)" as a source of rate of return. "Cumulative improvement cost for production" corresponds to "technical proficiencies" as described above.

$$\mathcal{G}(h_{S_i}(t)) = \frac{1}{k_2} \int S_i(t) dt \tag{7}$$

Definition 2.5. *Potential energy in production field* $\mathcal{F}$

$$\mathcal{F} = \int f(S_i(t), h_{S_i}(t)) dS_i, \quad {}^{\forall}0 \le t \le T \tag{8}$$

The deviation of the potential energy of production (the deviation of free energy) in the production field generates a rate of return. However, not all working costs necessarily lead to profit. Losses and disabled production costs (including inevitable revenue losses) are also included.

On the other hand, $\mathcal{H}(S_i, h_{S_i}(t))$ fluctuates with $h_T(S_i)$. Revenue is generated by deviations in $\Delta\mathcal{H}(S_i, h_{S_i}(t)))$. In summary, revenue is analogous to deviations in released energy.

The above discussion provides a physical interpretation of the Hamilton canonical production field [23].

Figure 5 shows a field $\mathcal{H}(S_i, h_{S_i}(t)))$ intersecting the production space. $\mathcal{H}(S_i, h_{S_i}(t)))$ moves on the constant surface toward the next intersection with elapsing time. The Hamilton-Jacobi equation defines the temporal and spatial variation of the field. "Completed (Return)" in Figure 5 indicates that revenue is sourced by completing a production operation.

Here the total rate of return is related to the potential energy of the total production cost as follows:

$$h_T(S_i) \approx \frac{d\mathcal{F}(S_i)}{dS_i} \tag{9}$$

Therefore, from Equations (9), (6) and (7), we can obtain total production cost corresponding to total rate of return as follows:

$$\frac{d\mathcal{F}(S_i)}{dS_i} \cong k_1 \frac{dS_i(t)}{dt} + \frac{1}{k_2} \int_0^t S_i(\tau) d\tau \tag{10}$$

where, $\frac{dS_i(t)}{dt}$ represents the cost variation per unit time and $\frac{1}{k_2} \int_0^t S_i(\tau) d\tau$ is the cumulative cost function. The constants k_1 and k_2 are referred to as the transform coefficients of the rate of return.

Thus, we find that the total rate of return is proportional to the cumulative cost function of the target product per hour. However, if the elasticity of cost to the rate of return per unit time is positive, the process increases the rate of return. In the opposite case (decreased throughput), the process decreases the rate of return.

When the company sets a semi-fixed price for a transaction cost $N(t)$ (depending on production equipment), the rate of return $S_i(t)$ depends on the production costs and develops a nonlinear characteristic. This trend represents the structure of the rate of return in the company. Although this study assumes specific equipment, a wide variety of equipment is used in real production processes.

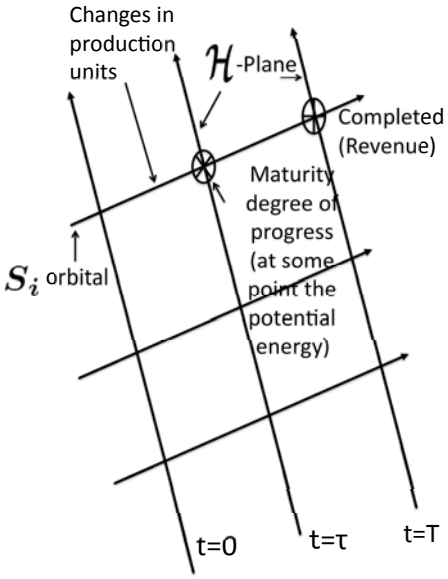

FIGURE 5. Potential energy fluctuation concept

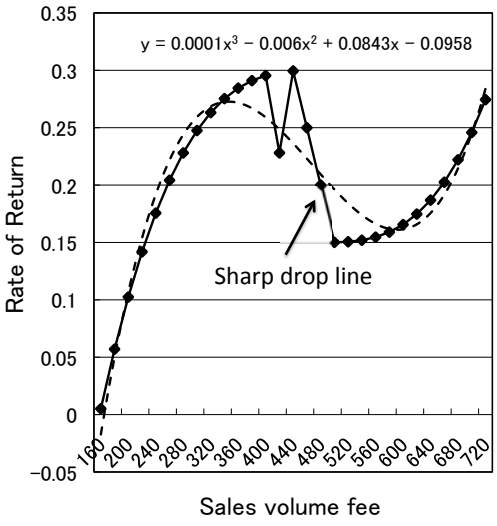

FIGURE 6. Rate of return on sales volume 1

3. **Potential Analysis for Production Process.** To apply a multimode vibration theory, we focus the potential field which is analogous to the mechanical field of physics [12]. In [19], we described the nonlinearity of production process in the potential field. We also propose a potential field for the production process (termed stochastic field in the production process) that is analogous to the mechanical field of physics [12]. The behavior of the production field is expressed as a partial differential equation describing a dynamic Hamilton-Jacobi field [23].

We also clarify the stable cycle conditions of the nonlinear characteristic parameter in the production field of the production process. To date, nonlinearity in the rate of sales return in the production process has not been reported. However, the data analyzed in this paper suggests that the rate of sales return can become nonlinear. The nonlinear element is the portion of production costs that cannot be directly attributed to sales.

Based on the rate of return on net sales, this paper mathematically analyzes nonlinearity in the rate of return on sales. The mathematical model is described by a van der Pol differential equation. Moreover, we clarify the stable cycle condition of the non-linear characteristic parameter in the production field of manufacturing process.

Figures 6-8 display graphs in which no significant difference is apparent between cumulative revenues related to production costs and revenues related to production throughput.

Figures 6-8 plot the rate of return on net sales of specific control equipment produced by some domestic enterprises from 1996 through 1998. The rate of return on sales gives rise to the nonlinear characteristics.

The dashed line in the figures is the fitted curve representing the relationship between the rate of return on sales and sales volume fee. In the data, the return rate plummeted from 0.3 at a sales fee of 480 to 0.15 at a sales fee of 440 (see Figure 6). This sharp drop represents the relationship in Equation (17).

The resulting straight line appears in the vicinity of the phase transition and is equivalent to the oscillation point of the reference line in elements displaying nonlinear characteristics (such as the Esaki diode) [11].

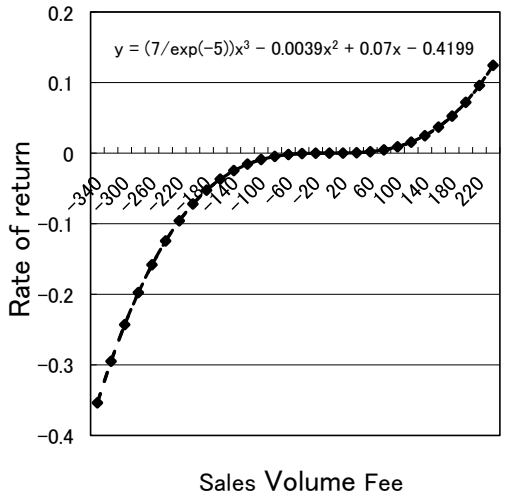

FIGURE 7. Rate of return on sales volume 2

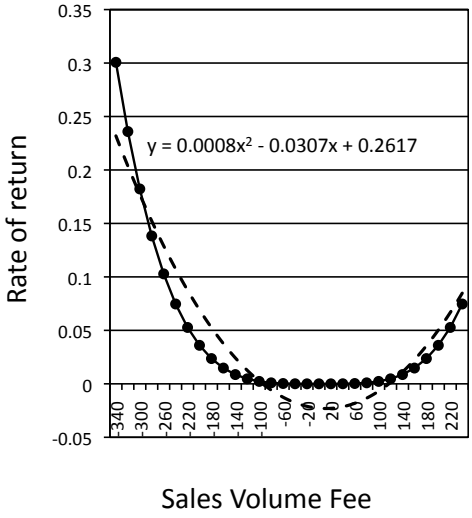

FIGURE 8. Rate of return on sales volume 3

TABLE 1. Set parameter values

	Type-1	Type-2	Type-3	Type-4	Type-5	Type-6	Type-7	Type-8	Type-9	Type-10
$\backslash\ K_S$	0.05	0.06	0.07	0.08	0.09	0.1	0.2	0.3	0.4	0.5
η_P	100	100	100	100	100	100	200	500	600	1000
η_S	10	10	10	10	10	100	100	250	300	500
η_S/η_P	0.1	0.1	0.1	0.1	0.1	1.0	0.5	0.5	0.5	0.5

We reported the phase transition about a production process in the previous paper [20]. K_S in Table 1 represents a phase transition coefficient (r), and both η_P and η_S represent a normalized constant.

Figure 9 illustrates the change in the phase transition factor when ΔD_n varies from -0.3 to $+0.3$, and $1/r$ indicates a boundary area in which phases are changed. In the horizontal axes of Figure 9, the area indicating $1/r$ is an area near $-0.133 < \Delta D_n < +0.1$.

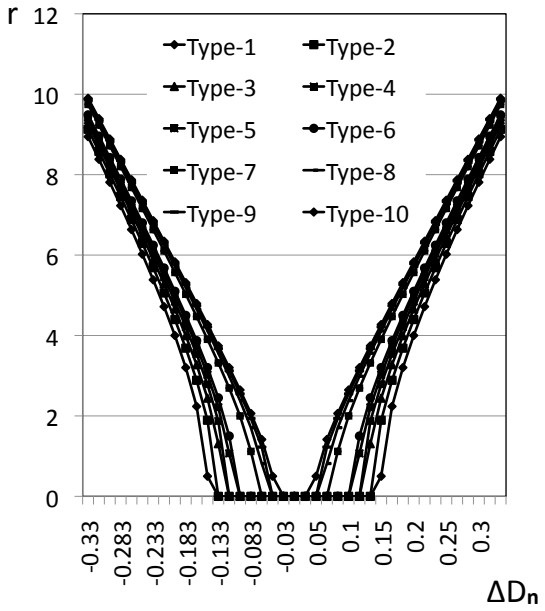

FIGURE 9. Phase transition coefficient for the STD of rate of return

The normalization constant was changed such that the normalization value of the rate-of-return deviation ΔD_n lies within the range -0.3 to $+0.3$. This is because by doing so, the relationship between the phase transition and potential becomes clear.

Accordingly, we think that it is important to know $|\Delta D_n|$, which is a critical point of the phase transition, and invest heavily into manufacturing operations in order to ensure the continued viability of the business.

4. **Multimode Vibrations in Electrical Circuits.** We apply the new degree-of-freedom oscillator solution proposed by Kuramitsu and Takase [22]. From a report on the Brayton-Moser theory, we apply a differential equation that describes two terminal elements (the number of coils, K; the number of capacities, J, along with some resistances) in an RLC circuit [21]. In addition, we need to introduce the scalar function $P(\boldsymbol{i}, \boldsymbol{v})$ of a mixed potential function. Thus, from these ideas and equations, Equations (12) and (13) can be established.

To establish the required differential equation, it should satisfy Kirchhoff's law in an electrical circuit. In a biological system, this differential equation needs to satisfy the Van der Pol equation.

In this paper, we analyze the production process using the multimode vibration.

Then, the mathematical model in the circuit under Kirchhoff's law is as follows. The mixed potential energy $P(\boldsymbol{i}, \boldsymbol{v})$ is generally as follows:

$$P(\boldsymbol{i}, \boldsymbol{v}) = F(\boldsymbol{i}) - G(\boldsymbol{v}) + H(\boldsymbol{i}, \boldsymbol{v}) \tag{11}$$

$$L_k(i_k)\frac{di_k}{dt} = \frac{\partial P(\boldsymbol{i}, \boldsymbol{v})}{\partial i_k} \tag{12}$$

$$C_j(v_j)\frac{dv_j}{dt} = -\frac{\partial P(\boldsymbol{i}, \boldsymbol{v})}{\partial v_j} \tag{13}$$

where, $F(\boldsymbol{i})$ is the current potential, $G(\boldsymbol{v})$ is the voltage potential, and $H(\boldsymbol{i}, \boldsymbol{v})$ is the loop potential. $k = 1, 2, \cdots, K$, $j = 1, 2, \cdots, J$, L_k is an inductance and C_j is a capacitor. i_k is the current flowing through the coil L_k, and v_j is the terminal voltage of C_j capacity.

Then, the energy is derived as follows [17]:

$$F(i) = \int v(i)di \tag{14}$$

$$G(v) = \int i(v)dv \tag{15}$$

where the power is almost zero, i.e., $F(\boldsymbol{i}) = G(\boldsymbol{v}) = 0$ [17].

Therefore, according to the averaging method, the equations for the generating systems are as follows:

$$L_k(i_k)\frac{di_k}{dt} = \frac{\partial P(\boldsymbol{i}, \boldsymbol{v})}{\partial i_k} = \sum_{j=1}^{J} \Gamma_{kj} v_j \tag{16}$$

$$C_j(v_j)\frac{dv_j}{dt} = -\frac{\partial P(\boldsymbol{i}, \boldsymbol{v})}{\partial v_j} = -\sum_{k=1}^{K} \Gamma_{kj} i_k \tag{17}$$

where, Γ_{kj} denotes 0, +1, −1. Equations (16) and (17) are lossless LC circuit model equation. By solving Equations (16) and (17), we obtain as follows [17]:

$$i_k(t) = \sum_{m=1}^{M} d_{mk} r_m \cos(\varphi_m t + \theta_m) \tag{18}$$

$$v_k(t) = \sum_{m=1}^{M} d'_{mk} r_m \cos(\varphi_m t + \theta_m) \tag{19}$$

where, r_m, θ_m are any constant, φ_m is a eigenfrequency of the system (Mode frequency), and M is the total number of modes. Then, d_{mk} and d'_{mk} are satisfied as follows:

$$\sum_{k=1}^{K} L_k d_{mk} d_{lk} = \sum_{j=1}^{J} C_j d'_{mj} d'_{lj} = \delta_{ml} I_m \tag{20}$$

$$\sum_{k=1}^{K} \sum_{j=1}^{J} \Gamma_{kj} d_{mk} d'_{lj} = \delta_{ml} \varphi_m I_m \tag{21}$$

In case of $F(i) = G(i) \neq 0$, the solution is derived as follows [17]:

$$i_k(t) = \sum_{m=1}^{M} d_{mk} r_m \cos \psi_m(t) \tag{22}$$

$$v_j(t) = \sum_{m=1}^{M} d'_{mk} r_m \cos \psi_m(t) \tag{23}$$

where, $\psi_m(t) = \varphi_m t + \theta_m$.

We construct a mathematical model of the production flow process being used in the production field using the multimode vibration theory. Figure 14 represents a production flow process, which has six stages (S1-S6) in this case, is a commercial process for the production of control equipment that is ultimately delivered to the customer. Figure 11 shows an example of three working stages of the production flow process. An oscillation circuit is connected to each stage.

Assumption 1. *The characteristics of production structure.*

- *1. The production structure is nonlinear.*

- *2. The production structure is a closed structure, i.e., the production flow process is cyclic.*

The item-1: The main factors in deciding whether or not to construct the equipment depend on (1) the value of the equipment in the marketplace and (2) the appropriate throughput for that equipment.

These factors are important because the product must satisfy the market demand and provide value for its users. Because the product depends on demand distribution and throughput to provide value for the users, the production structure has nonlinear characteristics.

The item-2 in Assumption 1 is clearly satisfied because the structure is continuous over a period in this production flow process [12]. This oscillator circuit corresponds to the delay at each stage of the production process [18]. A part of the equipment is produced at each stage with the production process moving from one stage to the next, and the final product is produced at the final stage in Figure 11. The variables in the mathematical model of the production process correspond to the variables of the electrical circuit as follows:

The current variable $i_k(t)$ corresponds to the production density $S(t)$, the voltage $v_k(t)$ corresponds to the rate of return $h(t)$, and both the inductance $L(t)$ and conductance $C(t)$ correspond to the throughput having nonlinear characteristics.

Instead of the current, the production density is dynamic at each stage of the production process. In the same way, instead of the voltage, the rate of return varies because the current also varies while flowing through an electrical circuit. Therefore, the rate of return corresponds reasonably well with the voltage. The throughput, which corresponds to both the inductance and conductance, is an index for evaluating the stability of the production process. It corresponds to the nonlinear elements of the circuit.

5. **Stability Evaluation of the Production Flow Process Using Multimode Vibration.** In Figure 10, the mathematical model of the production process is rewritten using the circuit equation, i.e., we obtain the following:

$$L_{12}\frac{di_{12}}{dt} = v_{11} - v_{22} \tag{24}$$

$$L_{23}\frac{di_{23}}{dt} = v_{22} - v_{33} \tag{25}$$

$$L_{34}\frac{di_{34}}{dt} = v_{33} - v_{44} \tag{26}$$

$$L_{41}\frac{di_{41}}{dt} = v_{44} - v_{11} \tag{27}$$

$$C_1\frac{dv_{11}}{dt} + \frac{1}{L_1}\int v_{11}dt + i_{11} = i_{41} - i_{12} \tag{28}$$

$$C_2\frac{dv_{22}}{dt} + \frac{1}{L_2}\int v_{22}dt + i_{22} = i_{12} - i_{23} \tag{29}$$

$$C_3\frac{dv_{33}}{dt} + \frac{1}{L_3}\int v_{33}dt + i_{33} = i_{23} - i_{34} \tag{30}$$

$$C_4\frac{dv_{44}}{dt} + \frac{1}{L_4}\int v_{44}dt + i_{44} = i_{34} - i_{41} \tag{31}$$

In the analysis of such simple coupling, Takase discusses the multimode vibration analysis in terms of average potential energy [17]. Kuramitsu et al. have certified that the structure is derived by the Van der Pol equation [21, 22].

Moreover, the data gathered from the production flow process indicates that all stages correlate with each other. Thus, in general, according to the method proposed by Takase and Kuramitsu, Figure 11 indicates the production flow process using the circuit diagram of Figure 10 [21, 22]. Here, "osc" in Figure 11 indicates the working-time delay at each stage in the production process.

If virtual stages "$1'$" and "$6'$" are added, we can apply an analytical method for the target system that describes the lattice-shaped oscillator group studied by Takase and Kuramitsu for biological phenomena [17, 21]. Here $L_X \neq L_Y$ and stage C can be referred to as a virtual coupling stage.

Moreover, the current $(i_{i,j})$ corresponds the rate of return $(h_{i,j})$, and the voltage $(v_{i,j})$ corresponds to the production density $(S_{i,j})$.

In the coupling stage C in Figure 13, we can obtain

$$L_Y \frac{di_{Y_{i,j}}}{dt} = v_{i,j} - v_{i+1,j} \tag{32}$$

$$C\frac{dv_{i,j}}{dt} + \frac{1}{L_X}\int v_{i,j}dt + i_{i,j} = i_{X_{i,j-1}} - i_{X_{i,j}} + i_{Y_{i-1,j}} - i_{Y_{i,j}} \tag{33}$$

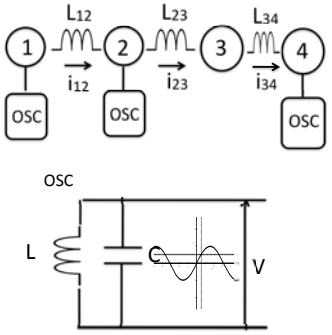

FIGURE 10. Circuit diagram

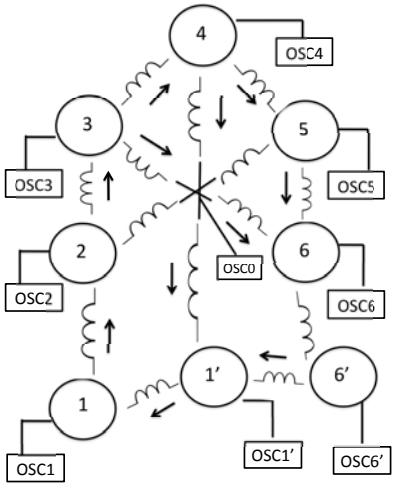

FIGURE 11. Production flow process modeled like an electrical circuit

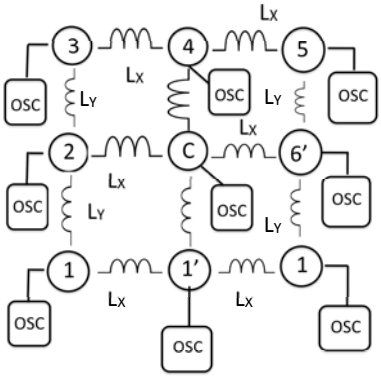

FIGURE 12. Modification of the production flow process given in Figure 11

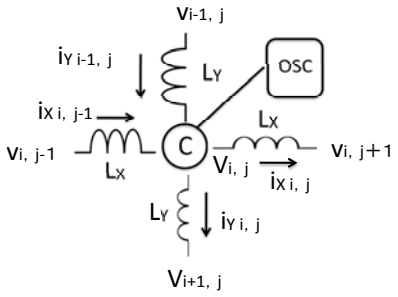

FIGURE 13. Circuit diagram expanded at the virtual stage C

Therefore, this solution is

$$S_{i,j}(t) = \sum_{l=1}^{3}\sum_{k=1}^{3} r_{lk}(t)_3P_{il} \cdot {}_3P_{jk} \sin\Big(w_{il}t + \theta_{jk}(t)\Big) \tag{34}$$

Any kind of combination mode [3 × 3] is a problem regardless of whether it is stable or not in multimode vibration. In the final product equipment, the issue is whether different stages synchronize or not because the synchronization process is the optimal (most appropriate) method.

In the case of coupling [e.g., (1′, OSC1′), (6′, OSC6′)], combining the previous stage mode and coupling mode or combining the final process mode and coupling mode produces slightly different throughput depending on the stage position, i.e., we obtain the following [21]:

$$({}_3P_{pC} \cdot {}_3P_{q1'})^2 + ({}_3P_{pC} \cdot {}_3P_{q6'})^2 = 1 \tag{35}$$

where, $p = 1, \cdots, 6$ and $q = 1, \cdots, 6$.

One stage complements the other; thus, a stable multivibration mode can be established by minimizing the average potential energy.

Table 7 and Table 8 indicate the production times and volatilities at each stage of the production flow process, respectively; these tables indicate "synchronization with preprocess". If Equations (32), (33), and (34) are established, the synchronous vibration mode is possible.

6. **Production Flow System.** Figure 14 shows a production process that is termed as a production flow process. This production process is employed in the production of

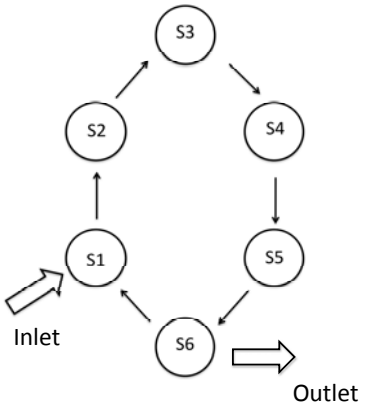

FIGURE 14. Production flow process

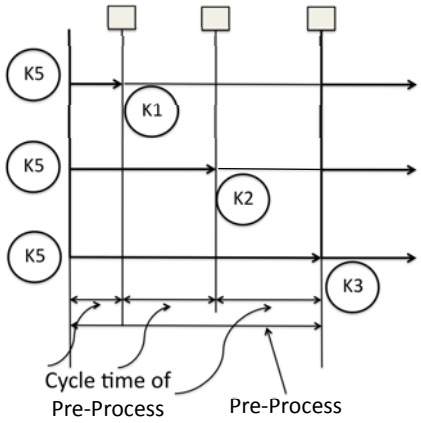

FIGURE 15. Previous process in production equipment

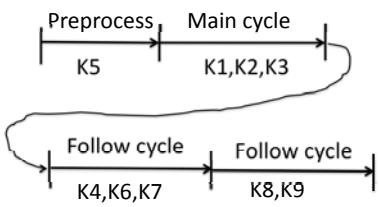

FIGURE 16. "Synchronization-with-preprocess" method in production equipment

control equipment. In this example, the production flow process consists of six stages. In each step S1-S6 of the production process, materials are being produced.

The direction of the arrows represents the direction of the production flow. In this process, production materials are supplied through the inlet and the end-product is shipped from the outlet.

7. **Analysis of the Test-Run Results.** Table 2 shows a comparison table of the working time for the production method of the Test-run1-3.

- (Test-run1): Each throughput in every process (S1-S6) is asynchronous, and its process throughput is asynchronous. Table 3 represents the production time (min) in each process. The volatilities of K3 and K8 increase due to the delay of K3 and K8 in Table 4. K3 and K8 of workers in Table 3 indicate the delay propagation of working time through S1-S6 stages. Table 4 represents the volatility in each process performed by workers. Table 3 represents the target time, and the theoretical throughput is given by $3 \times 199 + 2 \times 15 = 627$ (min).

  In addition, the total working time in stage S3 is 199 (min), which causes a bottleneck. Figure 17 is a graph illustrating the measurement data in Table 3, and it represents the total working time for each worker (K1-K9). The graph in Figure 18 represents the volatility data for each working time in Table 3.
- (Test-run2): Set to synchronously process the throughput.

  The target time in Table 5 is 500 (min), and the theoretical throughput (not including the synchronized idle time) is 400 (min). Table 6 represents the volatility data of each working process (S1-S6) for each worker (K1-K9).
- (Test-run3): Introducing a preprocess stage, the process throughput is performed synchronously with the reclassification of the process. The theoretical throughput (not including the synchronized idle time) is 400 (min) in Table 7. Table 8 represents the volatility data of each working process (S1-S6) for each worker (K1-K9).

TABLE 2. Correspondence between the table labels and the test run number

	Table Number	Production process	Working time	STD
Test-run1	Table 3	Asynchronous process	627 (min)	0.29
Test-run2	Table 5	Synchronous process	500 (min)	0.06
Test-run3	Table 7	Synchronous-with-preprocess	470 (min)	0.03

TABLE 3. Total production time at each stages for each worker (asynchronous)

	WS	S1	S2	S3	S4	S5	S6
K1	15	20	20	25	20	20	20
K2	20	22	21	22	21	19	20
K3	10	20	26	25	22	22	26
K4	20	17	15	19	18	16	18
K5	15	15	20	18	16	15	15
K6	15	15	15	15	15	15	15
K7	15	20	20	30	20	21	20
K8	20	29	33	30	29	32	33
K9	15	14	14	15	14	14	14
Total	145	172	184	199	175	174	181

TABLE 4. Volatility of Table 3

K1	1.67	1.67	3.33	1.67	1.67	1.67
K2	2.33	2	2.33	2	1.33	1.67
K3	1.67	3.67	3.33	2.33	2.33	3.67
K4	0.67	0	1.33	1	0.33	1
K5	0	1.67	1	0.33	0	0
K6	0	0	0	0	0	0
K7	1.67	1.67	5	1.67	2	1.67
K8	4.67	6	5	4.67	5.67	6
K9	0.33	0.33	0	0.33	0.33	0.33

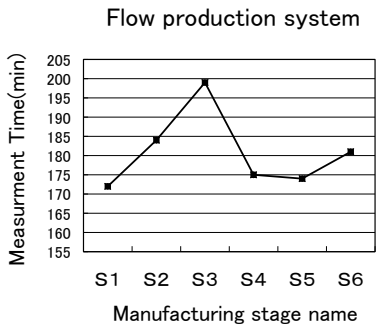

FIGURE 17. Total production time of each stage by each worker

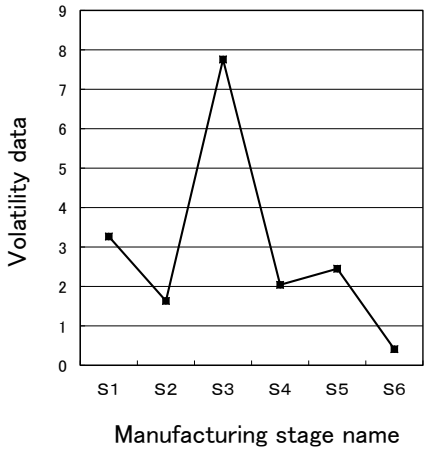

FIGURE 18. STD data of each worker at each stage

TABLE 5. Total production time at each stage by each worker (synchronous)

	WS	S1	S2	S3	S4	S5	S6
K1	20	18	19	18	18	18	18
K2	20	18	18	18	18	18	18
K3	20	21	21	21	21	21	21
K4	*16	13	11	11	13	13	13
K5	*16	16	16	17	17	16	16
K6	*16	18	18	18	18	18	18
K7	20	14	14	13	14	14	13
K8	20	22	22	22	22	22	22
K9	20	20	20	20	20	20	20
Total	168	165	164	163	166	165	164

TABLE 6. Volatility of Table 5

K1	0.67	0.33	0.67	0.67	0.67	0.67
K2	0.67	0.67	0.67	0.67	0.67	0.67
K3	0.33	0.33	0.33	0.33	0.33	0.33
K4	1	1.67	1.67	1	1	1
K5	0	0	0.33	0.33	0	0
K6	0.67	0.67	0.67	0.67	0.67	0.67
K7	2	2	2.33	2	2	2.33
K8	0.67	0.67	0.67	0.67	0.67	0.67
K9	1.67	1.67	1.67	1.67	1.67	1.67

From this result, the idle time must be set at 100 (min). Based on the above results, the target theoretical throughput ($T_s^{'}$) is obtained using the "synchronization-with-preprocess" method. This goal is

$$\begin{aligned} T_s \sim\ & 20 \times 6\,(\text{First cycle}) + 17 \times 6\,(\text{Second cycle}) \\ & + 20 \times 6\,(\text{Third cycle}) + 20\,(\text{Previous process}) + 8\,(\text{Idol-time}) \\ & = 370\,(\text{min}) \end{aligned} \tag{36}$$

The full synchronous throughput in one stage (20 min) is

$$T_s{}' = 3 \times 120 + 40 = 400\,(\text{min}) \tag{37}$$

The throughput becomes about 10% reduction in result. Therefore, the "synchronization-with-preprocess" method is realistic in this paper, and it is recommended the "synchronization-with-preprocess" method in the flow production system [14].

Now, we manufacture one equipment at 3 cycle. For maintaining the throughput of 6 units/day, the production throughput is as follows.

TABLE 7. Total production time at each stage for each worker (synchronous-with-preprocess), K5 (*): Preprocess

	WS	S1	S2	S3	S4	S5	S6
K1	20	18	19	18	18	18	18
K2	20	18	18	18	18	18	18
K3	20	21	21	21	21	21	21
K4	16	13	11	11	13	13	13
K5	16	*	*	*	*	*	*
K6	16	18	18	18	18	18	18
K7	16	14	14	13	14	14	13
K8	20	22	22	22	22	22	22
K9	20	20	20	20	20	20	20
Total	148	144	143	141	144	144	143

TABLE 8. Volatility of Table 7, K5: Previous process

K1	0.67	0.33	0.67	0.67	0.67	0.67
K2	0.67	0.67	0.67	0.67	0.67	0.67
K3	0.33	0.33	0.33	0.33	0.33	0.33
K4	1	1.67	1.67	1	1	1
K5	*	*	*	*	*	*
K6	0.67	0.67	0.67	0.67	0.67	0.67
K7	0.67	0.67	1	0.67	0.67	1
K8	0.67	0.67	0.67	0.67	0.67	0.67
K9	0	0	0	0	0	0

In Table 7, the working times of the workers K4, K7 show shorter than others. However, the working time shows around target time.

Next, we manufacture one piece of equipment in three cycles. To maintain a throughput of six units/day, the production throughput must be as follows:

$$\frac{(60 \times 8 - 28)}{3} \times \frac{1}{6} \simeq 25\,(\mathrm{min}) \tag{38}$$

where the throughput of the preprocess is set as 20 (min). In (38), "28" represents the throughput of the preprocess plus the idle time for synchronization. "8" is the number of processes and the total number of all processes is "8" plus the preprocess. "60" is given by 20 (min) $\times$ 3 (cycles).

Here, the preprocess represents the working until the process itself is entered. To eliminate the idle time after classification of the processes in advance, this preprocess was introduced. In Figure 15, for example, it represents the termination of the operation of step K5 during the preprocess. By making the corresponding step K5 to be the preprocess, there are eight remaining processes. When performing the 3 cycles in Figure 15, the first cycle is $\{\mathrm{K1}, \mathrm{K2}, \mathrm{K3}\}$, the second cycle is $\{\mathrm{K4}, \mathrm{K6}, \mathrm{K7}\}$, and the third cycle is $\{\mathrm{K8}, \mathrm{K9}\}$.

After completion of the third cycle, the workers start producting the next product. That is, the first production process starts the first cycle. By adopting the preprocess cycle, the third cycle is adopted in a parallel process.

At this time, the theoretical throughput (T_s) is as follows.

Here, the preprocess is adopted in test-run3 only.

The results are as follows. Here, the trend coefficient, which is the actual number of pieces of equipment/the target number of equipment, represents a factor that indicates the degree of the number of pieces of production equipment.

Test-run1: 4.4 (pieces of equipment)/6 (pieces of equipment) = 0.73,

Test-run2: 5.5 (pieces of equipment)/6 (pieces of equipment) = 0.92,

Test-run3: 5.7 (pieces of equipment)/6 (pieces of equipment) = 0.95.

Volatility data represent the average value of each test-run.

8. **Identification of Asynchronous and Synchronous Processes.** We identify the difference between asynchronous and synchronous processes using the multimode vibration theory to determine a matrix. The matrix is derived as follows: the matrix $\boldsymbol{A}^{'}$, which

is a condition for coexistence with multimode vibration, is given as follows:

$$\boldsymbol{A} = \begin{bmatrix} a_{11} & \cdots & a_{1N} \\ \vdots & \ddots & \vdots \\ a_{N1} & \cdots & a_{NN} \end{bmatrix} \tag{39}$$

Equation (39) is a symmetric matrix of $[N \times N]$, (40). However, we use a skew-symmetric matrix of $[6 \times 9]$ in this paper.

$$\boldsymbol{A} = \begin{bmatrix} a_{11} & \cdots & a_{16} \\ \vdots & \ddots & \vdots \\ a_{91} & \cdots & a_{96} \end{bmatrix} \tag{40}$$

The matrix $\boldsymbol{A}^{'}$, which is a condition for coexistence with multimode vibration, is given as follows:

$$\boldsymbol{A}' = \begin{bmatrix} a_{ll} & a_{ll'} \\ a_{l'l} & a_{l'l'} \end{bmatrix} \tag{41}$$

If $\boldsymbol{A}^{'} > 0$, it is well known that the two vibration modes l, $l^{'}$ coexist [21].

Next, for the matrix of (41), we count the number of instances of (1) $\boldsymbol{A}^{'} < 0$, (2) $\boldsymbol{A}^{'} = 0$, and (3) $\boldsymbol{A}^{'} > 0$ for the matrix of (41) using the measurement data retrieved from Table 3, Table 5, and Table 7.

Figure 19 uses the manpower data of Table 3 to produce a diagram for the evaluation of the positive, negative, and zero matrices using any four data values. For example, we pick up the first two values from the first row and the first two values from the second row of Figure 19.

$$\boldsymbol{A}' = \begin{bmatrix} 20 & 20 \\ 22 & 21 \end{bmatrix} \tag{42}$$

By calculating the above matrix, $\boldsymbol{A}^{'} = 20 \times 21 - 20 \times 22 = -20 < 0$. The value is changed in the positive or negative direction from the standard in the asynchronous process. The greater the change is, the greater the process becomes asynchronous.

20	20	25	20	20	20
22	21	22	21	19	20
20	26	25	22	22	26
17	15	19	18	16	18
15	20	18	16	15	15
15	15	15	15	15	15
20	20	30	20	21	20
29	33	30	29	32	33
14	14	15	14	14	14

FIGURE 19. Matrix of production process data provided in Table 3

18	19	18	20	20	20
18	18	18	20	20	20
21	21	21	20	20	20
13	11	11	20	20	20
16	16	17	20	20	20
18	18	18	20	20	20
14	14	13	20	20	20
22	22	20	20	20	20
25	25	25	20	20	20

FIGURE 20. Matrix of production process data provided in Table 5

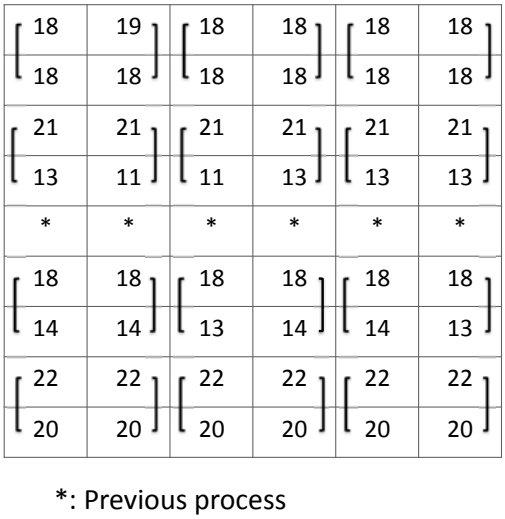

FIGURE 21. Matrix of production process data provided in Table 7

This calculation is shown as Table 9. In our test runs, Test-run1 is an asynchronous process, Test-run2 is synchronous process, Test-run3 is the synchronous-with-preprocess, i.e., the measurement data in Table 3 indicates the data for an asynchronous case and it takes the time to work. With regard to Test-run 1-3, the ranking of throughput is Test-run $1 < 2 < 3$. We should explore the appropriate throughput based on the synchronization-with-preprocess case.

TABLE 9. Number of (a) $\boldsymbol{A}' > 0$, (b) $\boldsymbol{A}' = 0$, (c) $\boldsymbol{A}' < 0$

	(1) Asynchronous	(2) Synchronous	(3) Synchronous-with-preprocess
(a) $\boldsymbol{A}' > 0$	5	2	2
(b) $\boldsymbol{A}' = 0$	1	7	8
(c) $\boldsymbol{A}' < 0$	6	3	2

9. **Conclusions.** In this study, we indicated that stable regions of nonlinearity of the production process correspond to the range of phase transitions. On the basis of manpower data, we proposed an evaluation method for production process that decreases or increases the throughput, using multimode vibration theory. We quantitatively identified the process as being either asynchronous or synchronous.

An oscillation circuit corresponds to the delay at each stage of the production process. For example, if a delay occurs at working stage S1, it propagates to the next stage, S2. This phenomenon observed in an electrical circuit corresponds well to the production process. However, the production process does not resonate like an electrical circuit. The transmission of vibration reduces the throughput of the entire process. Using multimode vibration theory, we could identify whether the production process was asynchronous or synchronous. In the future, this theory can be effective for evaluating different production processes.

REFERENCES

[1] M. E. Mundel, *Improving Productivity and Effectness*, Prentice-Hall, NZ, 1983.

[2] R. E. Haber, A. Gajate, S. Y. Liang, R. Haber-Haber and R. M. del Toro, An optimal fuzzy controller for a high-performance drilling process implemented over an industrial network, *International Journal of Innovative Computing, Information and Control*, vol.7, no.3, pp.1481-1498, 2011.
[3] K. Nishioka, Y. Mizutani, H. Ueno et al., Toward the integrated optimization of steel plate production process – A proposal for production control by multi-scale hierarchical modeling –, *Synthesiology*, vol.5, no.2, pp.98-112, 2012.
[4] L. Sun, X. Hu, Y. Fang and M. Huang, Knowledge representation for distribution problem in urban distribution systems, *International Journal of Innovative Computing, Information and Control*, vol.6, no.9, pp.4145-4156, 2010.
[5] L. Hu, D. Yue and J. Li, Availability analysis and design optimization for repairable series-pararell system with failure dpendencies, *International Journal of Innovative Computing, Information and Control*, vol.8, no.10(A), pp.6693-6705, 2012.
[6] S. Hiiragi, *The Significance of Shortening Lead Time from a Business Perspective*, http://merc.e.u-tokyo.ac.jp/mmrc/dp/index.html, MMRC, University of Tokyo, 2012 (in Japanese).
[7] N. Ueno, M. Kawasaki, H. Okuhira and T. Kataoka, Mass customization production planning system for muli-process, *Journal of the Faculty of Management and Information Systems, Prefectural University of Hiroshima*, no.1, pp.183-192, 2009 (in Japanese).
[8] C. Zhang and H. Wang, State-space based study stability, bullwhip effect and total costs in two-stage supply chains, *International Journal of Innovative Computing, Information and Control*, vol.8, no.5(A), pp.3399-3410, 2012.
[9] H. Kondo and K. Nisinari, Modeling stock congestion in production management, *Reports of RIAM Symposium, Mathematics and Physics in Nonlinear Waves*, no.20, pp.146-149, 2008 (in Japanese).
[10] T. Chen and Y.-C. Lin, A collaborative fuzzy-neural approach for internal due date assignment in a wafer fabrication plant, *International Journal of Innovative Computing, Information and Control*, vol.7, no.9, pp.5193-5210, 2011.
[11] T. Kamibayashi and S. Matsuda, Analysis of a negative resistance oscillator – Quasi-Harmonic Oscillator –, *Bulletin of the Shiga University*, pp.56-66, 1973.
[12] K. Shirai and Y. Amano, Production density diffusion equation propagation and production, *IEEJ Transactions on Electronics, Information and Systems*, vol.132-C, no.6, pp.983-990, 2012.
[13] K. Shirai and Y. Amano, A study on mathematical analysis of manufacturing lead time – Application for deadline scheduling in manufacturing system, *IEEJ Transactions on Electronics, Information and Systems*, vol.132-C, no.12, pp.1973-1981, 2012.
[14] K. Shirai, Y. Amano and S. Omatu, Synchronous and asynchronous models for the evaluation of manufacturing process, *International Journal of Innovative Computing, Information and Control*, Paper Submission, 2013.
[15] K. Shirai, Y. Amano and S. Omatu, Power-law distribution of rate-of-return deviation and evaluation of cash flow in a control equiopment manufacturing company, *International Journal of Innovative Computing, Information and Control*, vol.9, no.3, pp.1095-1112, 2013.
[16] H. Tasaki, *Thermodynamics – A Contemporary Perspective (New Physics Series)*, Baifukan, Co., LTD., 2000.
[17] F. Takase, Multi-mode vibration in the group of transmitters coupled lattice, *KURENAI: Kyoto University Research Information Repository*, vol.413, pp.10-29, 1981.
[18] K. Shirai, Y. Amano and S. Omatu, Propagation of working-time delay in production, *International Journal of Innovative Computing, Information and Control*, vol.10, no.1, pp.169-182, 2014.
[19] K. Shirai and Y. Amano, Nonlinear characteristics of the rate of return in the production process, *International Journal of Innovative Computing, Information and Control*, vol.10, no.2, pp.601-616, 2014.
[20] K. Shirai, Y. Amano and S. Omatu, Consideration of phase transition mechanisms during production in manufacturing processes, *International Journal of Innovative Computing, Information and Control*, vol.9, no.9, pp.3611-3626, 2013.
[21] M. Kuramitsu and Y. Nishikawa, A mathematical analysis of self-organization in electrical circuits, *The Society of Instrument and Control Engineers*, vol.29, no.10, pp.899-904, 1990.
[22] M. Kuramitsu and H. Takase, Analysis of multi-degree-of-freedom oscillator with average potential, *The Journal of IEICE*, vol.J66-A, no.4, pp.336-343, 1983.
[23] K. Kitahara, *Nonequilibrium Statistical Physics*, Iwanami, Co. LTD., 1997.